

Minimally disruptive laser-induced breakdown in water

E. N. Glezer, C. B. Schaffer, N. Nishimura, and E. Mazur

Department of Physics and Division of Engineering and Applied Sciences, Harvard University, Cambridge, Massachusetts 02138

Received July 17, 1997

We produce minimally disruptive breakdown in water by using tightly focused 100-fs laser pulses and demonstrate the potential use of this technique in microsurgery of the eye. Using time-resolved imaging and piezoelectric pressure detection, we measure the magnitude and speed of propagation of the pressure wave produced in the breakdown. Compared with breakdown with longer pulses, here there is a much lower energy threshold for breakdown of $0.2 \mu\text{J}$, a smaller shock zone diameter ($11 \mu\text{m}$ for $1\text{-}\mu\text{J}$ pulses), and consistent energy deposition. © 1997 Optical Society of America

Laser-induced breakdown is widely used in ophthalmic surgery.^{1,2} The breakdown generates a hot plasma that expands with hypersonic velocity and drives a shock wave.³ The shock wave decays into an acoustic wave as its supersonic propagation slows to the speed of sound.⁴ Precise confinement of the disrupted region in tissue is limited by size of the plasma and the extent of the shock zone (region of supersonic expansion) where the high pressure causes damage.⁵ Most clinical applications employ 10-ns pulses from a Nd:YAG laser with pulse energies greater than 1 mJ, which produce shock zones greater than 1 mm in diameter.^{1,2} The large shock zone limits surgical precision and can cause collateral tissue damage. Furthermore, unwanted energy deposition can occur in any absorptive tissue outside the focal region; an important consequence is that photodisruptive laser surgery cannot be performed within 4 mm of the retina.¹ Several recent experiments have shown that using picosecond and femtosecond pulses reduces the required pulse energy and decreases the size of the region damaged by the shock wave.⁴⁻¹⁰

In this Letter we probe the limits of minimally disruptive breakdown induced by tightly focused 100-fs laser pulses. We use water as an experimental model for examining the breakdown and shock wave propagation.¹¹ To characterize the pressure wave produced by the breakdown we use time-resolved imaging and piezoelectric pressure detection. With the imaging we observe an ionized vapor bubble and an expanding spherical pressure wave. By measuring the rate of expansion we determine the size of the shock zone. The piezoelectric detection provides a sensitive technique and a large dynamic range for measuring the pressure at a distance of several millimeters. We measure the dependence of the pressure on the pulse energy and compare this dependence for 100-fs and 200-ps pulses.

Figure 1(a) shows the setup for time-resolved imaging of a cross section through the center of the spherical pressure wave front. A 100-fs, 800-nm-wavelength pump pulse from an amplified Ti:sapphire laser is focused by a 0.6-N.A. microscope objective in the middle of a 1-mm-thick water cell with thin glass windows. The resulting dynamics are illuminated by a time-delayed probe, which is a 100-fs, 400-nm-wavelength pulse, and imaged onto a CCD camera.

The 800-nm pump is blocked by a filter. We vary the time delay between the pump and the probe from 0 to 60 ns to monitor the expansion of the pressure wave front.

Figure 1(b) shows an image of the small vapor bubble and the pressure wave 35 ns after optical excitation by a $1\text{-}\mu\text{J}$ pulse. Figure 1(c) shows a larger bubble and a more visible pressure wave driven by a $14\text{-}\mu\text{J}$ pulse. Each of these figures was averaged over 30 CCD images to improve the image quality.

In Fig. 2 we plot the radial expansion of the pressure wave driven by 1-, 10-, and $30\text{-}\mu\text{J}$ pulses. The radii were measured to the outer edge of the pressure wave. Included for comparison is a line representing the propagation of sound in water ($1.48 \mu\text{m}/\text{ns}$). The expansion velocity (slope in the data) matches the speed of sound for all but the first fraction of a nanosecond. The shock zone has a diameter of 11, 17, and $20 \mu\text{m}$ for

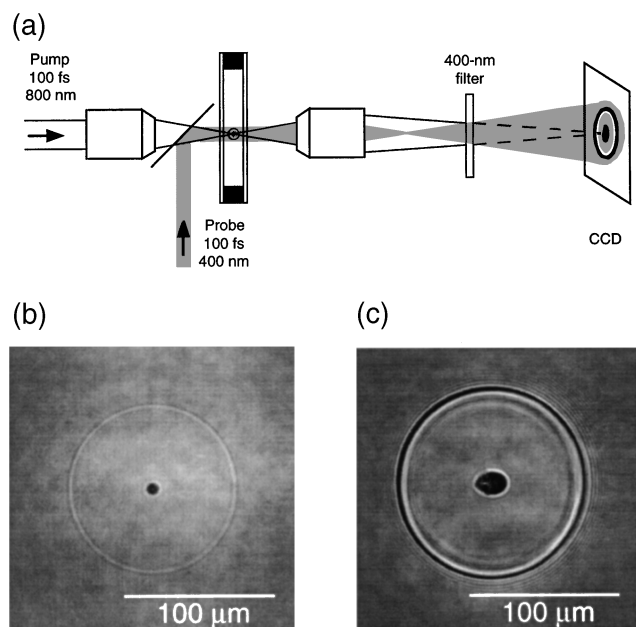


Fig. 1. (a) Time-resolved imaging setup for observing the dynamics of laser-induced breakdown in water. Small vapor bubbles and expanding pressure waves photographed 35 ns after optical excitation by 100-fs, 800-nm laser pulses of (b) $1\text{-}\mu\text{J}$ and (c) $14\text{-}\mu\text{J}$ energy.

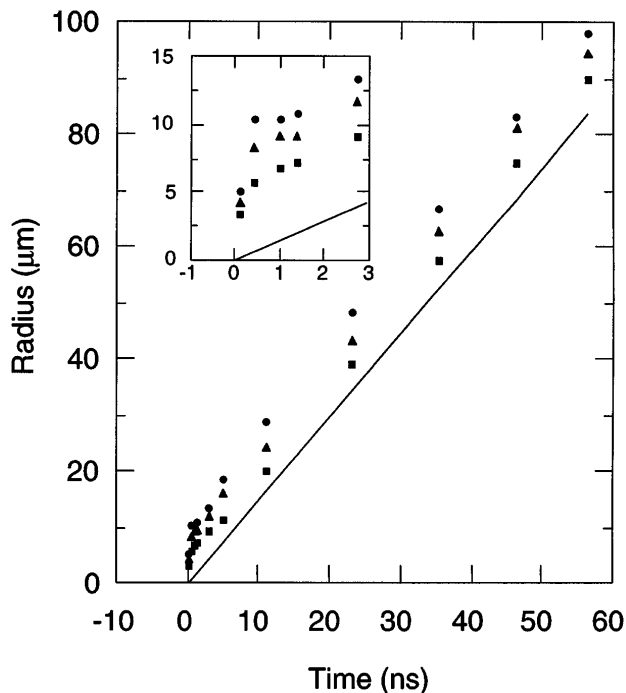


Fig. 2. Radial expansion of the pressure wave driven by 1- μJ (filled squares), 10- μJ (filled triangles), and 30- μJ (filled circles) pulses. The radii were measured to the outer edge of the pressure wave. The line represents propagation of sound in water ($1.48 \mu\text{m}/\text{ns}$). The inset shows the first 3 ns of expansion from which the shock zone and initial expansion velocity are determined.

1-, 10-, and 30- μJ pulses, respectively. These findings are different from those from experiments with 40-ps pulses, in which the shock zone was found to extend to a 200–400- μm diameter for 25- μJ pulses.⁴ The expansion of the vapor bubble and the shock wave is extremely rapid. At 100 ps the vapor bubble diameter for 1- μJ pulses is already 7 μm . The initial diameter is determined by the 1- μm laser spot size, giving an expansion velocity of $\sim 30 \mu\text{m}/\text{ns}$, i.e., 20 times the speed of sound in water. Such an explosive expansion suggests that it is driven by megabar pressures. Despite the extreme initial conditions, the total deposited energy is much less than with longer pulses, and the shock zone is much smaller.

Figure 3(a) shows the setup for piezoelectric pressure detection. A 0.65-N.A. objective is used to focus laser pulses 100–200 μm inside a water cell containing a submerged piezoelectric sensor. We amplify the piezoelectric voltage and record the signal on a digital oscilloscope. Figure 3(b) shows the response of the sensor to a propagating pressure wave driven by a 100-fs, 1.8- μJ pulse. The oscillations correspond to several vibration modes of the sensor. The amplitude of the response increases with increasing energy, but the shape of the response changes only slightly. Using the height of the first peak, we measure the magnitude of the pressure in the wave as a function of input energy, shown in Fig. 4. We find a sharp threshold of 0.2 μJ for detecting a pressure wave, followed by a nearly linear increase of pressure with input energy. Figure 5 shows on a logarithmic scale the pressure

produced by 100-fs and 200-ps pulses over 3 orders of magnitude in laser pulse energy.¹² Above 10 μJ , the pressure produced by the 100-fs and 200-ps pulses is equal. In the range 10–100 μJ the logarithmic slope is 0.5, indicating that the pressure increases approximately as the square root of the input energy and that the deposited energy is proportional to the input energy.

With 200-ps pulses the breakdown occurs randomly in the vicinity of the threshold. In fact, no clear threshold exists. In the range 2–6 μJ an increasing percentage of the laser shots produce breakdown, with no breakdown below 2 μJ and breakdown on every shot above 6 μJ . In contrast, with 100-fs pulses there is little shot-to-shot variation in the pressure produced by the breakdown, even close to the threshold. Below 1 μJ the absorbed fraction of each pulse diminishes with decreasing incident energy but the breakdown occurs consistently from shot to shot. This difference in behavior occurs because the energy deposition for 100-fs pulses is initiated by multiphoton absorption, whereas the absorption of 200-ps pulses relies on absorbing impurities to generate the initial electrons.

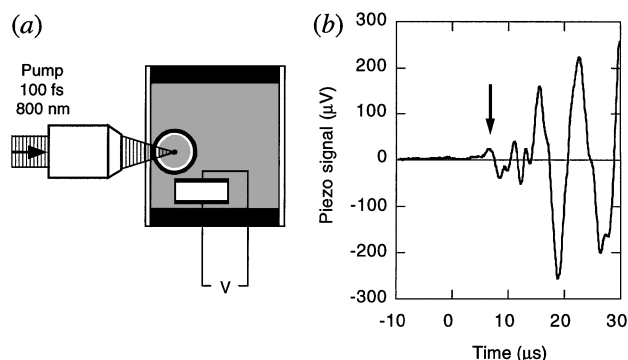


Fig. 3. (a) Water cell for piezoelectric pressure measurements. (b) Response of the piezoelectric sensor to the pressure wave produced by a 100-fs, 1.8- μJ pulse. The signal is averaged over 100 pulses. We use the amplitude of the first peak (arrow) as a measure of the pressure in the wave.

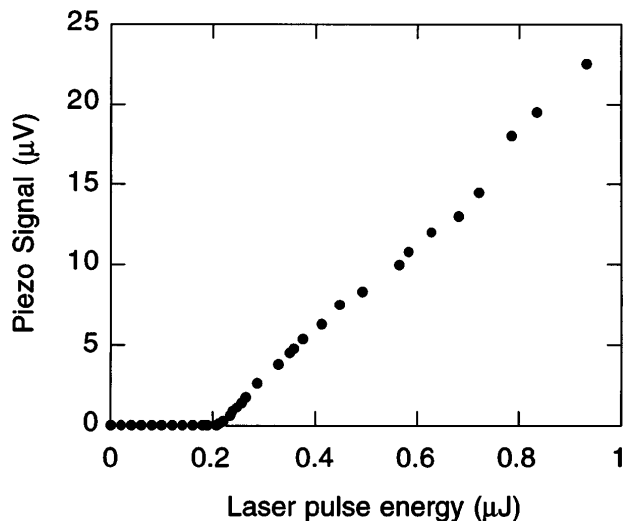


Fig. 4. Piezoelectric detection of the pressure wave produced by 100-fs laser-induced breakdown in water.

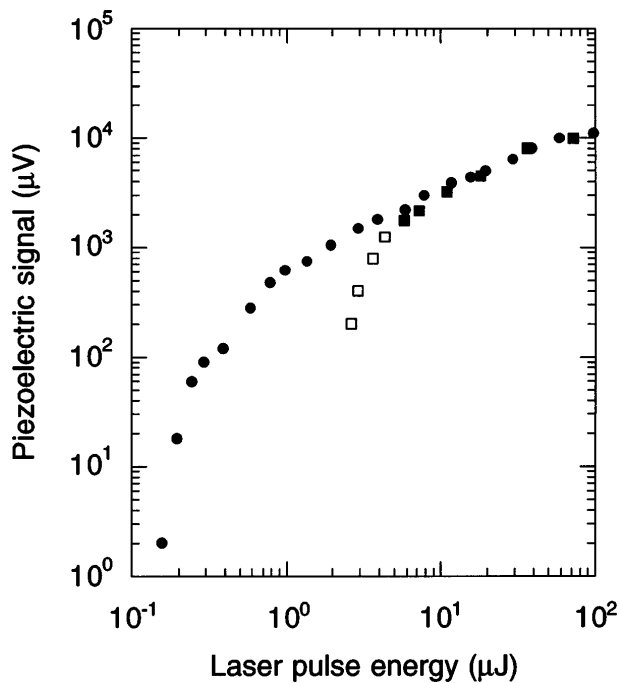


Fig. 5. Comparison of the pressure produced by 100-fs pulses (filled circles) and 200-ps pulses (squares) in water. Each point is averaged over 100 pulses. In the 200-ps data the open squares represent a range in pulse energy where some pulses produce no signal, whereas others significantly exceed the average.

For pulses with energies greater than $10 \mu\text{J}$ we find a transmission of 20% through the water sample, indicating that a larger fraction of the incident energy is absorbed. Assuming 80% absorption in this energy range, we can use the pressure measurements to extrapolate the absorption coefficient to smaller energies. The low pressure produced by 100-fs pulses near the $0.2\text{-}\mu\text{J}$ threshold indicates that it is possible consistently to deposit a small fraction of the incident energy—approximately 50 pJ —into the pressure wave, making it conceivable to photodisrupt biological tissue with subcellular precision.

A unique advantage of femtosecond pulse breakdown is that the energy threshold is nearly independent of material properties and impurities and thus can be applied consistently to a variety of tissues. The $0.2\text{-}\mu\text{J}$ threshold for 100-fs pulse breakdown in water is similar to the $0.05\text{--}0.1\text{-}\mu\text{J}$ damage threshold observed in our experiments under similar focusing conditions in transparent solids such as glass, quartz, and sapphire.^{13–15}

In conclusion, we use tightly focused 100-fs, 800-nm laser pulses to produce breakdown in water. We image the nanosecond dynamics and measure the expansion of the resulting pressure wave. Using a piezoelectric sensor, we determine the dependence of the pressure on laser pulse energy over a large range and compare this dependence for 100-fs and 200-ps pulses. We find that, with 100-fs pulses focused by a 0.65-N.A. objective, $0.2\text{-}\mu\text{J}$ pulses are sufficient to create breakdown and launch a pressure wave. The

shock zone is greatly reduced compared with that obtained with longer pulses, reaching a radius of only $11 \mu\text{m}$ with $1\text{-}\mu\text{J}$ pulses. The strength of the pressure wave is consistently determined by the energy in the 100-fs pulse, unlike with 200-ps pulses, which produce inconsistent breakdown at energies near the threshold. These results demonstrate the potential advantages of using ultrashort laser pulses for microsurgery of the eye. The lower breakdown threshold and smaller shock zone would reduce the collateral tissue damage. The consistent breakdown near the threshold would allow microsurgery to be done with little energy and extreme precision.

References

1. J. M. Krauss and C. A. Puliafito, in *Laser Surgery and Medicine: Principles and Practice*, C. A. Puliafito, ed. (Wiley-Liss, New York, 1996), Chap. 8, p. 249.
2. R. F. Steinert and C. A. Puliafito, *The Nd:YAG Laser in Ophthalmology: Principles and Clinical Applications of Photodisruption* (Saunders, Philadelphia, Pa., 1985).
3. P. A. Barnes and K. E. Rieckoff, *Appl. Phys. Lett.* **13**, 282 (1968).
4. B. Zysset, J. G. Fujimoto, and T. F. Deutsch, *Appl. Phys. B* **48**, 139 (1989).
5. Later, a cavitation bubble forms on a microsecond time scale. The size and evolution of the cavitation bubble in corneal tissue are reported in X. H. Hu, L. Turi, and Z. Bor, *Lasers Surg. Med.* **15**, 91 (1994); T. Juhasz, G. A. Kastis, C. Suarez, Z. Bor, and W. E. Bron, *Lasers Surg. Med.* **17**, 1 (1995).
6. A. G. Doukas, A. D. Zweig, J. K. Frisoli, R. Birngruber, and T. F. Deutsch, *Appl. Phys. B* **53**, 237 (1991).
7. T. Juhasz, G. Kastis, C. Suarez, L. Turi, Z. Bor, and W. E. Bron, *Proc. SPIE* **2681**, 428 (1996).
8. A. Vogel, S. Busch, and U. Parlitz, *J. Acoust. Soc. Am.* **100**, 148 (1996).
9. D. X. Hammer, R. J. Thomas, G. D. Noojin, B. A. Rockwell, P. K. Kennedy, and W. P. Roach, *IEEE J. Quantum Electron.* **32**, 670 (1996).
10. C. P. Cain, G. D. Noojin, D. X. Hammer, R. J. Thomas, and B. A. Rockwell, *J. Biomed. Opt.* **2**, 88 (1997).
11. Water is a good basic model for studies of breakdown and shock wave propagation in tissue for two reasons: First, breakdown thresholds for femtosecond pulses differ little from one transparent material to another (see text). Second, shock dynamics are similar in water and tissue because tissue is composed largely of water and thus has nearly the same density, compressibility, and sound velocity. The similarity of the shock wave dynamics has been confirmed by experiments comparing water with bovine corneas [T. Juhasz, X. H. Hu, L. Turi, and Z. Bor, *Lasers Surg. Med.* **15**, 91 (1994)].
12. The data in Fig. 5 were taken by use of the magnitude of a later peak in the detector response, i.e., not the first peak, which was used in Fig. 4.
13. E. N. Glezer, M. Milosavljevic, L. Huang, R. J. Finlay, T.-H. Her, J. P. Callan, and E. Mazur, *Opt. Lett.* **21**, 2023 (1996).
14. E. N. Glezer and E. Mazur, *Appl. Phys. Lett.* **71**, 882 (1997).
15. The larger value of the energy threshold in water is likely due to spherical aberration introduced by focusing through a $180\text{-}\mu\text{m}$ -thick window in the water cell.